Desalination and Water Treatment
www.deswater.com
doi: 10.5004/dwt.2023.29615

298 (2023) 155–173
June

The adsorption behaviors of industrial dyes by natural mordenite: isotherm, kinetic, thermodynamic, and Box–Behnken design study

Khuloud A. Alibrahim

Department of Chemistry, College of Science, Princess Nourah bint Abdulrahman University, P.O. Box: 84428, Riyadh 11671, Saudi Arabia, email: kaalibrahim@pnu.edu.sa/dr.kbrahim@yahoo.com

Received 25 January 2023; Accepted 19 May 2023

ABSTRACT

The adsorption of two model dyes, methylene blue (MB) and Acid Red 97 (AR97), onto mordenite was examined in this study using an experimental design method. They used response surface modeling and a Box–Behnken surface statistical design to optimize the removal of dyes from aqueous solutions. Solution pH, the quantity of dyes, and the dose of mordenite were the three factors taken into consideration. The study discovered that the adsorption of methylene blue was significantly influenced by solution pH, with pH 10 having the best adsorption effectiveness. In contrast, pH 3 was discovered to be the ideal setting for Acid Red 97. Additionally, the scientists discovered that both dyes experienced chemisorption, which is a chemical reaction between the dye and the surface of the mordenite. The study also looked into how time, dosage, and pH affected the adsorption procedure. Further research into the impact of temperature revealed that higher temperatures resulted in greater adsorption effectiveness. The adsorption process for both dyes was endothermic and spontaneous, which is compatible with thermodynamic principles, which contend that chemical reactions are more likely to occur at higher temperatures. Compare the adsorption outcomes with various adsorbents. It was discovered that AR97 and MB had the best adsorption rates, respectively, of 1,212.76 mg and 559.8 mg/g. Overall, the study offers insightful information about the adsorption of dyes onto mordenite and emphasises the significance of taking a number of variables into account when designing an adsorption process, including solution pH, temperature, and dose.

Keywords: Mordenite; Methylene blue; Acid Red 97; Adsorption; Box–Behnken design

1. Introduction

The coloring industry is a significant and crucial sector globally. However, the wastewater generated from this industry poses a potential threat to the environment due to the wide range of colors present in it. Some of these dyes have been demonstrated to be mutagenic and carcinogenic, making them hazardous to wildlife. Moreover, individuals who come into contact with these dyes may experience adverse effects on their kidneys, liver, brain, reproductive system, and central nervous system. Therefore, it is crucial to prioritize the removal of dyes from the environment [1]. Inexpensive methods are being researched by scientists to remove toxic dyes from the aquatic environment. The textile industry alone is estimated to release around 100 tons of dyes and pigments into water streams annually [2,3]. Dyes and pigments are commonly used by various industries, such as plastics, textiles, cosmetics, pharmaceuticals, and paper, to add color to their finished products. The dyeing of textiles is a significant contributor to environmental pollution, and wastewater containing processed textile colors is becoming increasingly voluminous. Worldwide, the chemical industry utilizes over 7 × 105 tons of dyes annually, with 10%–15% of these released into waterways as

effluents, resulting in severe environmental contamination and harm to both aquatic and human life. The vast majority of the over ten thousand commercially available types of dyes are considered harmful. Moreover, due to their complex and highly persistent aromatic structures, most dyes tend to accumulate in nature [4,5].

Throughout human history, water has been one of the most essential resources for survival and progress. However, in recent decades, water contamination has become a serious environmental concern on a global scale, especially due to the presence of various toxins polluting marine systems [6]. Even in small concentrations, industrial dye contamination of ground and surface waters poses a threat to both human health and the health of other living organisms. Synthetic dyes are widely used by numerous industries, including those in textiles, paper, leather, plastics, cosmetics, rubber, printing, and dyeing [3,6].

Studies have shown that dyes are highly resistant and stable in aquatic environments, making their release into the environment a major source of hydrosphere contamination. The presence of dyes in water resources reduces sunlight penetration into deeper areas, disrupting the photochemical and biological processes of aquatic species. The discharge of dyes into carbon-based water bodies leads to reduced photosynthetic activity and dissolved oxygen levels, in addition to having a carcinogenic effect. The accumulation of synthetic dyes and their byproducts in marine organisms and sediments can substantially reduce the biochemical oxygen demand and chemical oxygen demand levels in water supplies. With the annual production of over 100,000 types of dyes totalling about 7,000,000 tonnes and their negative impact on water resources, it is crucial and inevitable to remove dye pollution from wastewater [3,7].

Various techniques such as ozonation, flocculation, membrane separation, aerobic or anaerobic treatment, coagulation, and adsorption have been employed to remove dyes from wastewater. Among these techniques, adsorption has been identified as a promising and effective method for treating wastewater containing dye pollutants due to its ease of use, low cost, quick regeneration, sludge-free operation, and lack of production of harmful and dangerous fumes [8,9].

The removal of dyes by activated carbon is influenced by several variables, including the concentration of the dyes, the mass of the activated carbon, the pH and temperature of the solution, and other factors. These variables can impact the adsorption capacity and kinetics of activated carbon and should be considered when designing an effective treatment process for dye-containing wastewater [10–12]. Optimizing experimental conditions for high removal efficiency through factor-by-factor optimization alone may not be sufficient. The use of experimental design approaches can enhance removal efficiency while requiring fewer experiments. Response surface methodology (RSM) is a powerful and widely used mathematical technique that is suitable for modeling and improving industrial processes and chemical reactions. It can be employed to optimize the experimental conditions for maximum dye removal efficiency while minimizing the number of experimental runs required [13]. The aim of optimization is to find the optimal value for each variable in the model developed through experimental design and analysis. Various response surface designs, such as central composite, complete factorial, Box–Behnken, and others, are employed in the optimization process. It has been demonstrated that Box–Behnken is more efficient for three-level designs than the central composite design but less efficient than the three-level complete factorial design. Additionally, Box–Behnken designs have the advantage of avoiding regions where all components are simultaneously at their maximum or minimum levels, which is beneficial in preventing studies conducted under challenging conditions that may result in unsatisfactory outcomes [14].

It is obvious that the goal of this study is to examine how methylene blue and Acid Red 97 behave in aqueous solutions after being absorbed by mordenite, a powerful and reasonably priced adsorbent. By integrating Box–Behnken design and response surface methods, the study also attempts to maximize the adsorptive removal of the two dyes from the aqueous solution utilizing mordenite (RSM). Solution pH, dye concentration, and mordenite mass ratio are all factors taken into account in this optimization. Based on preliminary study, these variables were chosen to reduce the non-significant contribution of other factors. RSM is a statistical method used to optimise the experimental settings, while the Box–Behnken design is a sort of experimental design that permits assessment of the primary effects of the components and their interactions. The study seeks to identify the ideal conditions for the adsorption of methylene blue and Acid Red 97 from the aqueous solution using mordenite by combining these two techniques. The findings of this study may offer crucial information on how these dyes behave and how well mordenite works as an adsorbent to remove them. In conclusion, the goal of this study is to examine how methylene blue and Acid Red 97 behave in aqueous solutions after being absorbed by mordenite, a potent and reasonably priced adsorbent. By integrating Box–Behnken design and RSM, the study attempts to improve the adsorptive removal of the two dyes from the aqueous solution using mordenite while taking into account the variables of solution pH, dye concentration, and mordenite mass ratio. The findings of this study may shed light on how these dyes behave as well as the efficiency of mordenite as an adsorbent for their removal.

2. Material and methods

2.1. Materials

In this study, analytical-grade substances were used, including mordenite, Acid Red 97, methylene blue, sodium hydroxide (NaOH), and hydrochloric acid (HCl) 37%, which were purchased from Sigma-Aldrich (Germany). Solutions were prepared in bi-distilled water.

2.2. Experimental design

To evaluate how the parameters being studied interact with each ot her and their impact on dye adsorption, the optimal number of tests was determined using the Box–Behnken design. A total of 17 experiments were carried out using a three-level, three-factorial Box–Behnken experimental

design. The factor levels were assigned –1 (low), 0 (central point) and 1 (high) codes. After conducting preliminary tests to identify the optimal parameters and establish the experimental domain, the solution pH (X_1), dye concentration (X_2), and modified orange residue (MOR) dose (X_3) were selected as the most influential parameters. Table 1 shows the Box–Behnken design levels for each parameter [15,16]. In order to develop the statistical experimental design and analyze the data collected, the trial software Design-Expert 8.0.7.1 was employed. The experimental data was then fitted to the second-order polynomial equation [Eq. (1)] using a manual regression method to identify the relevant model terms. The quadratic response model can be expressed as a combination of linear terms, square terms, and linear-by-linear interaction elements, and is as follows:

$$Y = \beta_0 + \sum \beta_i X_i + \sum \beta_{ii} X_{i2} + \sum \beta_i X_i^2 + \sum_i \sum_i \beta_{ij} X_i X_j + e_i \quad (1)$$

The response of interest, represented by the adsorption capacity of Acid Red 97 (q_e (AR97)) and the adsorption capacity of methylene blue (q_e (MB)), can be expressed as Y in the quadratic response model. The constant is denoted by β_0, while the slope or linear effect of the input factor X_i is represented by β_i. The linear-by-linear interaction effect between the input factors X_i and X_j is denoted by β_{ij}, and the quadratic effect of input factor X_i is represented by β_{ii}.

2.3. Adsorption experiments

To prepare the synthetic dyes, the required amount of each dye was dissolved in distilled water to create stock solutions. These stock solutions were then diluted to form subsequent solutions with a concentration of 3.125 mol. For the sorption studies, a series of 25 mL bottles were prepared with the dye solution, each having a varying initial concentration (X_2 = 1.3 × 10^{-3} to 3.4 × 10^{-3} mol) and the corresponding mass of MOR (X_3 = 0.01 to 0.1). To achieve the desired pH, NaOH or HCl (1 M) solutions were used to adjust the solutions (X_1 = 3 to 10) for both dyes. The mixtures were then shaken for 5 to 100 min at a speed of 300 rpm at room temperature to assess the effect of time. Finally, the effect of temperature on the adsorption process was investigated by conducting the adsorption process at different temperatures. After the sorption tests, the samples were centrifuged at 3,400 rpm for 10 min to remove any remaining dyes. The remaining dye concentrations were then measured using a DR 5000 HACH UV-Vis spectrophotometer (Germany). The adsorption capacity of the dyes at equilibrium (in mmol/g) was determined by calculating the quantity of adsorbate per gram of adsorbent, using the following equations:

$$q_e = \frac{(C_0 - C_e)V}{m} \quad (2)$$

$$\%R = \frac{(C_0 - C_t)}{C_0} \times 100 \quad (3)$$

3. Results and discussion

3.1. Experimental results

Table 1 presents the preparatory conditions and experimental findings for the reactions being studied. The adsorption of methylene blue (q_e (MB)) and Acid Red 97 (q_e (AR97)) resulted in adsorption capacity values ranging from 0.10 to 1.71 mmol/g for methylene blue and 1.60 to 1.75 mmol/g for Acid Red 97. The highest values of 1.71 and 1.75 mmol/g were achieved with a MOR of 0.01 g/25 mL, but in an acidic medium for AR97 and a basic medium for methylene blue. The observed results can be explained by the change in surface charge of MOR and the protonation of functional groups on the dye molecules in response to changes in pH of the solutions. In an acidic solution (AR97), protonation of activated carbon leads

Table 1
Variance analysis for methylene blue adsorption

Source	Sum of squares	df	Mean square	*F*-value	*p*-value	
Model	2.80	9	0.3114	15.04	0.0009	Significant
A-pH	0.0160	1	0.0160	0.7715	0.4089	
B-Conc.	2.35	1	2.35	113.35	<0.0001	
C-Dose	0.1188	1	0.1188	5.73	0.0478	
AB	0.2096	1	0.2096	10.12	0.0155	
AC	0.0003	1	0.0003	0.0131	0.9119	
BC	0.1102	1	0.1102	5.32	0.0544	
A^2	0.0000	1	0.0000	0.0020	0.9656	
B^2	0.0001	1	0.0001	0.0060	0.9405	
C^2	1.602E-06	1	1.602E-06	0.0001	0.9932	
Residual	0.1450	7	0.0207			
Lack of fit	0.1450	3	0.0483	1.226E+06	<0.0001	Significant
Pure error	1.577E-07	4	3.943E-08			
Cor. total	2.95	16				

R^2 = 0.958, R^2_{adj} = 0.882.

to an increase in interaction with anionic dye molecules, which facilitates the adsorption process. In basic media, the cell surface of MOR carries a net negative charge. Consequently, with higher pH values, the significance of the interactions between the adsorbent and cationic dye (methylene blue) increases, facilitating the adsorption process. Regression analysis was performed to fit the response functions to the experimental data. The results showed that the MOR dosage had a negative impact on the adsorption of both dyes, while the dye concentration had a positive impact. Additionally, the pH of the solution had a negative effect on the adsorption of methyl orange, whereas it had a positive effect on the adsorption of methylene blue (Fig. 1).

3.2. Analysis of variance

To determine the significance of the curvature in the responses, an analysis of variance (ANOVA) was conducted with a confidence level of 95%. The effect of a factor refers to the change in the response caused by a change in the level of that factor. This is often referred to as a main effect, as it is related to the key points of interest in the experiment. The significance of the model and its terms' parameters was determined using Fisher's statistical test *F*-test, with significance being indicated by Prob. > *F* values lower than 0.05. The ANOVA was used to assess the significance of the quadratic model's fitting for both responses, with the results presented in Tables 1 and 2. Based on the ANOVA results, the equations accurately represented the actual relationship between each response and the significant variables. The ANOVA study revealed that all three parameters (solution pH, dye concentration, and MOR dose) have a significant impact on the adsorption yield. However, the mass ratio of activated carbon had a negative effect on the adsorption yield for both dyes, regardless of the dye concentration in the solution. The correlation coefficients indicate that the dye concentration in solution had a greater impact on the adsorption of AR97 compared to MB. In contrast, the mass ratio of activated carbon had a greater impact on the adsorption of MB compared to AR97. The ANOVA analysis also showed that the pH of the solution had a positive impact on the adsorption of MB and a negative impact on the adsorption of AR97. This result can be attributed to the fact that AR97 is an anionic dye, whereas MB is a cationic dye. At higher pH levels, there are more negatively charged surface sites available, making it easier for the dye to be adsorbed. However, at lower pH values, the presence of excess H^+ ions inhibit the adsorption process. In the case of the anionic dye AR97, the opposite behavior was observed. The linear-by-linear interaction analysis indicated that the most significant interactions for MB adsorption were those between dye concentration and activated carbon mass ratio (X_2X_3). For AR97 adsorption, the strongest relationships were found between solution pH and dye concentration, as well as between solution pH and activated carbon mass ratio (X_1X_3 and X_1X_2, respectively). Regarding the quadratic effect contribution, the mass ratio had the greatest influence on MB adsorption, while solution pH had the greatest influence on AR97 adsorption [17].

3.3. Diagnostic model

Fig. 2 presents the actual and expected values obtained from the regression coefficients of the proposed models. The comparison between experimental data values and those produced by the model (*Y* predicted) (*Y* experimental) can be observed in the figure. As shown in Fig. 2, most of the data points were evenly distributed along the straight line, indicating a strong correlation between the experimental and projected response values. Based on the results, the "R^2" values were in reasonable agreement with the "R^2_{adj}" values, and the "R^2" values were higher than the "R^2_{adj}" values. This suggests that the models fit the experimental data reasonably well and that the inclusion of additional

Table 2
Variance analysis for the adsorption of Acid Red 97

Source	Sum of squares	df	Mean square	*F*-value	*p*-value	
Model	0.0857	9	0.0095	4.00	0.0405	Significant
A-pH	0.0200	1	0.0200	8.43	0.0229	
B-Conc.	0.0464	1	0.0464	19.54	0.0031	
C-Dose	0.0125	1	0.0125	5.26	0.0555	
AB	0.0007	1	0.0007	0.3136	0.5929	
AC	0.0011	1	0.0011	0.4711	0.5146	
BC	0.0021	1	0.0021	0.8753	0.3806	
A^2	0.0008	1	0.0008	0.3472	0.5742	
B^2	4.475E-07	1	4.475E-07	0.0002	0.9894	
C^2	0.0020	1	0.0020	0.8591	0.3848	
Residual	0.0166	7	0.0024			
Lack of fit	0.0166	3	0.0055	3.772E+06	<0.0001	Significant
Pure error	5.880E-09	4	1.470E-09			
Cor. total	0.1023	16				

R^2 = 0.911, R^2_{adj} = 0.788.

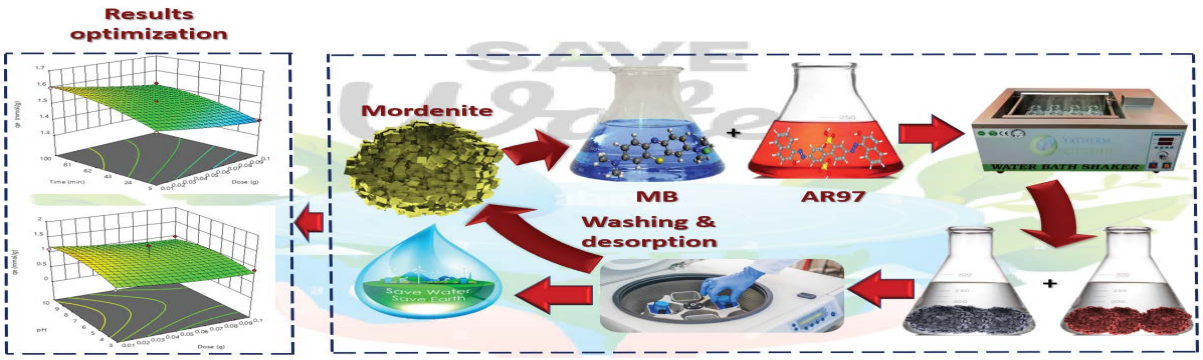

Fig. 1. Schematic diagram of adsorption Acid Red 97 and methylene blue.

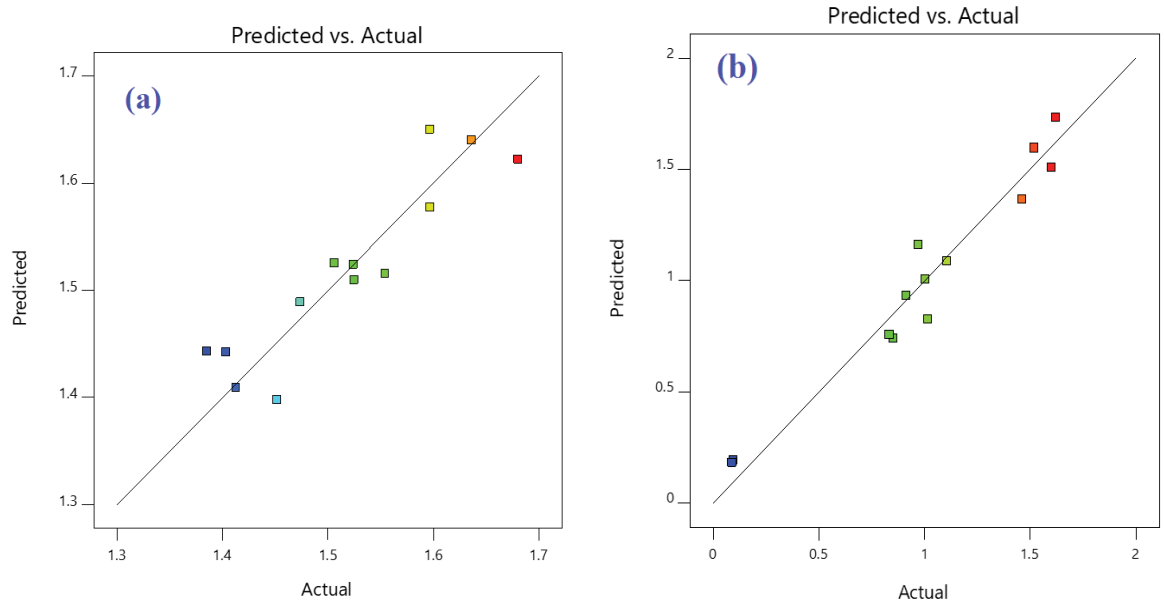

Fig. 2. Predicted vs. actual values for (a) Acid Red 97 and (b) methylene blue adsorption.

terms in the models did not result in overfitting. The models developed were able to accurately predict more than 95% of the reactions, indicating that the terms included in the models were sufficient to produce reliable predictions. The desirability value for the removal of both dyes was 1, indicating that it was desirable. The desired ranges for each response were reflected in this function, with a range of zero to one, indicating the least to the most desirable values, respectively. For the removal of MB, the desirability value was achieved at pH 10, MOR 0.02 g/25 mL, and an anticipated sorption capacity of 1.72 mmol/g. On the other hand, for the removal of AR97, the maximum desirability value was obtained at pH 3 and a dose of 0.02 g/25 mL for a sorption capacity of 1.75 mmol/g. The respective *F*-values of the MB and AR97 adsorption models were 15.04 and 4, indicating their significance. The probability that the high model *F*-value was due to noise was only 0.09% for MB adsorption and 4.05% for AR97 adsorption, confirming the importance of the proposed models. However, both dyes showed a lack of fit with *F*-values of 1.226E+06 for MB sorption and 3.772E+06 for AR97 solubility, indicating the importance of the lack of fit in both cases.

3.4. Response surface analysis

Figs. 3 and 4 depict the 3D response surface plots generated by statistical procedures for different combinations. The significant interactions for MB adsorption were found to be dye concentration/mass ratio of activated carbon and dye concentration/solution pH. For AR97 adsorption, the significant interactions were solution pH/MOR mass ratio and solution pH/dye concentration. As shown in Fig. 3a, MB adsorption increased with increasing dye concentration and decreasing MOR mass ratio. In Fig. 3, it can be observed that solution pH has a positive effect on the removal of MB at both low and high dye concentrations. The maximum MB adsorption was achieved at high dye concentration and high solution pH. Fig. 3b indicates that at low dye concentrations, the mass ratio of MOR has a stronger influence on MB adsorption. However,

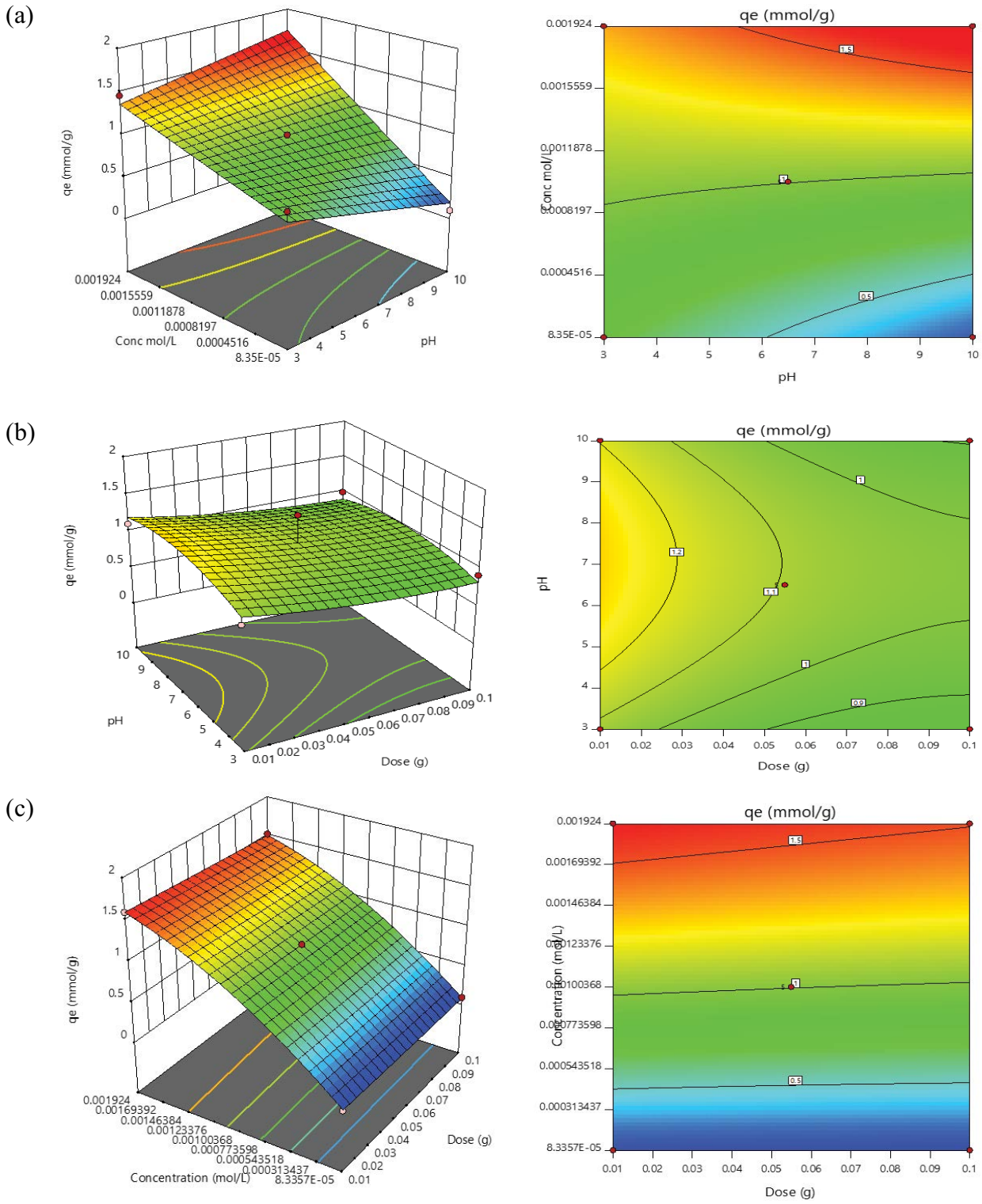

Fig. 3. Plots of the response surfaces and contours for methylene blue adsorption (a–c).

at low activated carbon mass ratios, the dye concentration has a lesser impact on dye removal. Fig. 3c shows that MB adsorption increases with a decrease in the mass ratio of MOR and an increase in dye concentration.

In Fig. 4 it can be observed that AR97 adsorption is highly sensitive to solution pH. Fig. 4a shows that AR97 adsorption at low solution pH is strongly influenced by its concentration in solution. Furthermore, the impact of solution pH is

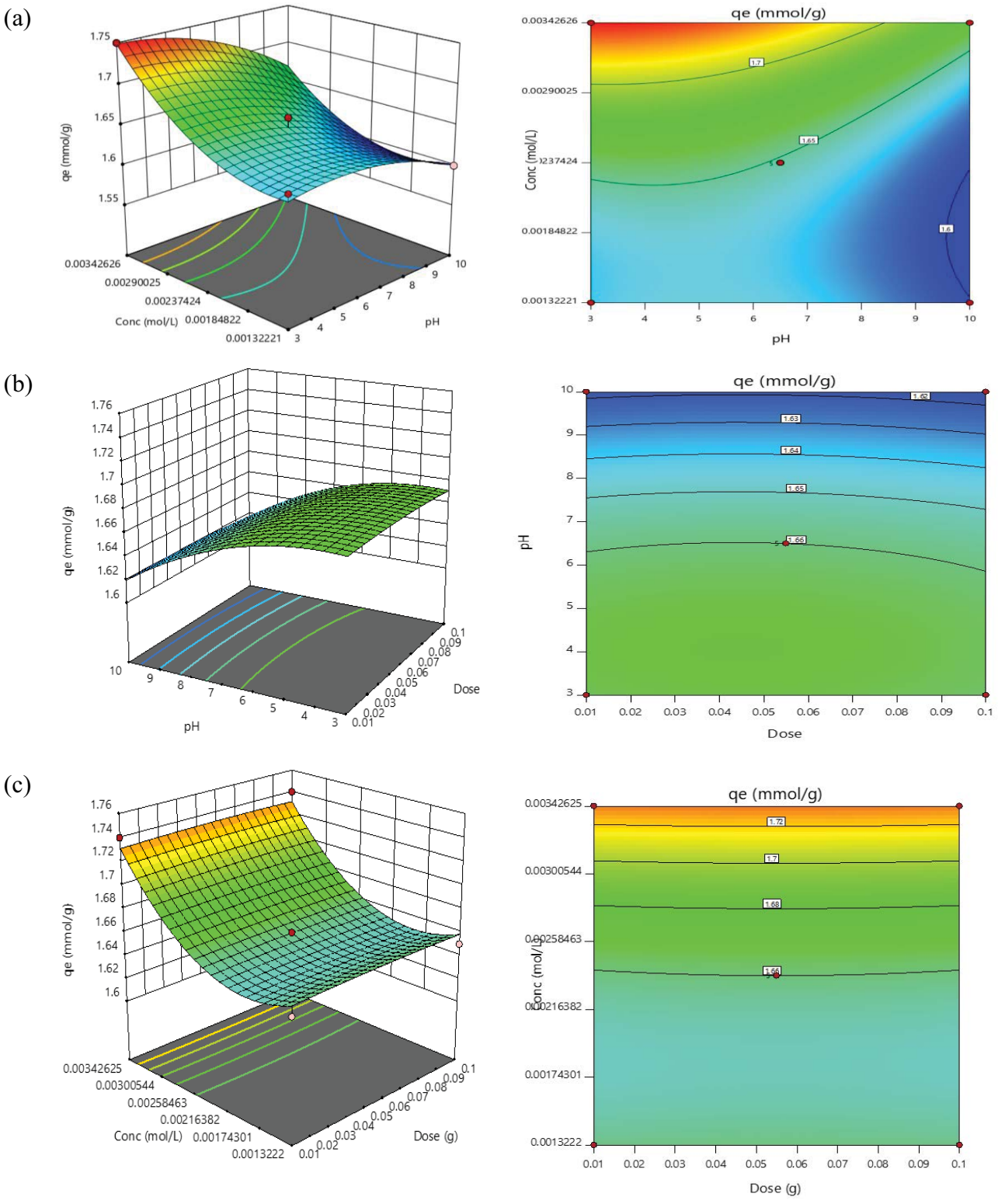

Fig. 4. Plots of the response surfaces and contours for the adsorption of Acid Red 97 (a–c).

more pronounced at high dye concentrations. At high dye concentrations and low solution pH, the highest adsorption capacity of AR97 was observed, as shown in Fig. 4a while Fig. 4b indicates a significant relationship between the mass ratio of MOR and solution pH. When the solution pH is high, an increase in MOR is associated with an increase in AR97 adsorption. However, at low solution pH, the opposite trend was observed. The highest AR97 adsorption

was achieved with a MOR dose of 0.2 g/25 mL and a solution pH of 3. In contrast, Fig. 4c shows an increase in AR97 adsorption at low MOR and high dye concentrations.

While approved the kinetic data using Box–Behnken design by using X_1, X_2, X_3, and time, dose, and pH, respectively. Fig. 5 illustrates the results kinetically that approved that optimum condition for AR97 was time 100 min, pH 3, and time dose 0.01 g. A *F*-value of 157.89 for AR97 suggests that the model is significant, while *p*-values lower than 0.0500 suggest that model terms are significant. While for MB the optimum condition at pH 10, time 100 min, and dose 0.01 g. Model significance is shown by the model's *F*-value of 123.03. Model terms are significant when their *p*-values are lower than 0.0500 (Tables 3 and 4).

3.5. Adsorption isotherm

In order to evaluate how the adsorbate is distributed from the liquid phase to the solid phase up until equilibrium under regulated (fixed) conditions, it is necessary to use an instrument for adsorption isotherm studies [12,18]. Various types of adsorption isotherms have been used to determine the maximum adsorption capacity, adsorption mechanism, adsorbent affinity, and nature of the reaction, whether monolayer or multilayer adsorption. Four widely used models, namely Langmuir [19], Freundlich [20], Dubinin–Radushkevich [21], and Temkin [22], were applied to fit the experimental data. Table 3 shows the isotherm models used in the study. The Langmuir model is based on three assumptions: monolayer adsorption, identical adsorption sites, and the independence of the adsorption of any molecule on the active sites of the adsorbent from occupancy at its surrounding sites (Table S1). On the other hand, the Freundlich model is an empirical equation that assumes the active sites on the adsorbent are heterogeneous and that multilayer accumulation is possible [5,23,24].

As shown in Table 5 and Fig. 6, the adsorption isotherm for both dyes were fitted to the Langmuir model based on the R^2 values obtained. Additionally, the adsorption process was found to be chemisorption as the adsorption energy for both dyes was greater than 8 kJ/mol.

The Langmuir, Freundlich, Dubinin–Radushkevich, and Temkin models all have non-linear forms, and these non-linear forms are crucial because they enable the fitting of experimental data to the models, which can reveal crucial details about a system's adsorption behavior.

Regression analysis frequently use the non-linear versions of these models to find the model parameters and fit experimental isotherm data to the models. These variables can subsequently be utilised to compute crucial adsorption features as the surface coverage, adsorption capacity, and strength of the adsorbate–adsorbent interaction.

Additionally, it is possible to compare the adsorption behavior of diverse systems and evaluate how different experimental conditions affect adsorption by using the non-linear forms of these models. Using this knowledge, adsorption procedures for many industrial applications can be optimized. In conclusion, it should be noted that the non-linear versions of the Langmuir, Freundlich, Dubinin–Radushkevich, and Temkin models are crucial because they enable the fitting of experimental data to the models and offer crucial details about a system's adsorption behavior. They may be applied to improve adsorption processes for diverse industrial applications, compute significant adsorption parameters, and compare the adsorption behavior of various systems.

3.6. Kinetics

Adsorption kinetics studies are important for designing adsorption systems and gaining a comprehensive understanding of the adsorption reaction pathway, equilibrium time, and identifying potential steps that may influence the sorbate and adsorbent interaction at the liquid–solid interface [11,24,25]. These studies are crucial for researchers to establish practical industrial adsorption systems. Four widely used kinetics models, namely the pseudo-first-order rate equation (PFORE) [26], pseudo-second-order rate equation (PSORE) [27], intraparticle diffusion (IPD) [28], and Elovich models [29], were used to manage the outcome data and determine the best-fitted kinetics model representing the kinetics adsorption process. The interaction time impact and its order in terms of adsorption kinetics were evaluated using the PFORE, PSORE, IPD, and Elovich models in an effort to represent the AR97 and MB diffusion process and their controlling step (Table S2).

The PSORE model assumes that the adsorption process is controlled by a chemisorption mechanism involving the sharing or transferring of electrons between the adsorbate and adsorbent surface, while the PFORE model assumes that the rate of the adsorption process is directly proportional to the variation between q_e and q_t. Linearized fitting was used to assess the model's applicability, as shown in Fig. 7. Comparing the computed (R^2) values for the two models presented in Table 6, it is clear that the results of AR97 and MB adsorption onto MOR were not fit with the PFORE model and are better suited with the PSORE model. Theoretically, there are three significant phases involved in the migration of the adsorbate from the bulk solution to the adsorbent (solid) surface. The first stage involves the bulk solution's AR97 and MB molecules being externally transferred to the MOR surface (film diffusion). In addition, the molecules AR97 and MB diffuse through the MOR pores to occupy the adsorptive sites (intraparticle diffusion). Lastly, a consistent distribution of anionic AR97 and MB molecules on the MOR surface is linked to a potent connection between those molecules and the negatively charged MOR [30–32].

In comparison to their linear equivalents, non-linear adsorption kinetics models such the pseudo-first-order, pseudo-second-order, intraparticle diffusion, and Elovich models have the following advantages:

Non-linear models are often more accurate in fitting experimental data than linear models, especially when the data is complicated or noisy; reveals information about the adsorption mechanism: non-linear models can reveal details about the adsorption mechanism, such as the rate constant and the activation energy, which can be utilized to understand the adsorption process; predictive ability: non-linear models can be used to forecast system behaviour based on its present condition. This is especially helpful for improving adsorption processes; non-linear models are

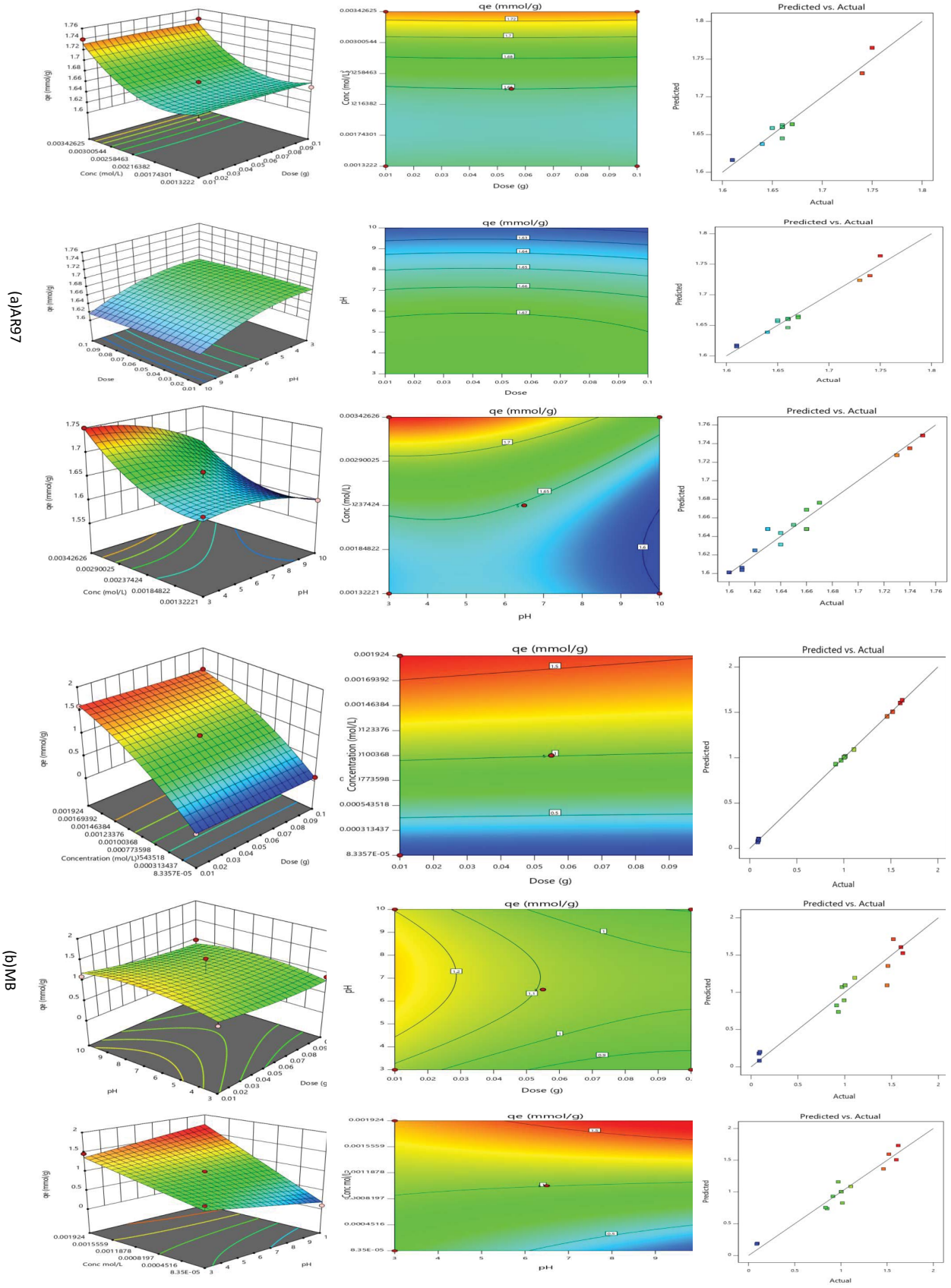

Fig. 5. Response surface plots and contour plots for the effects of conc., dose, pH on (a) Acid Red 97 and (b) methylene blue adsorption.

Table 3
Analysis of variance for Acid Red 97 adsorption as the effect of time

Source	Sum of squares	df	Mean square	*F*-value	*p*-value	
Model	0.1604	9	0.0178	157.89	<0.0001	Significant
A-Dose	0.0176	1	0.0176	155.69	<0.0001	
B-Time	0.0811	1	0.0811	718.57	<0.0001	
C-pH	0.0543	1	0.0543	480.49	<0.0001	
AB	0.0000	1	0.0000	0.2423	0.6332	
AC	0.0007	1	0.0007	6.12	0.0329	
BC	0.0001	1	0.0001	0.9260	0.3586	
A^2	0.0003	1	0.0003	2.65	0.1348	
B^2	0.0056	1	0.0056	49.34	<0.0001	
C^2	0.0005	1	0.0005	4.28	0.0653	
Residual	0.0011	10	0.0001			
Lack of fit	0.0011	3	0.0004			
Pure error	0.0000	7	0.0000			
Cor. total	0.1616	19				

Table 4
Analysis of variance for methylene blue adsorption as the effect of time

Source	Sum of squares	df	Mean square	*F*-value	*p*-value	
Model	0.1074	9	0.0119	123.03	<0.0001	Significant
A-Dose	0.0179	1	0.0179	184.69	<0.0001	
B-Time	0.0288	1	0.0288	297.07	<0.0001	
C-pH	0.0558	1	0.0558	575.53	<0.0001	
AB	9.060E-06	1	9.060E-06	0.0934	0.7662	
AC	0.0006	1	0.0006	6.04	0.0338	
BC	0.0000	1	0.0000	0.3766	0.5531	
A^2	0.0003	1	0.0003	2.75	0.1284	
B^2	0.0032	1	0.0032	32.70	0.0002	
C^2	0.0006	1	0.0006	5.87	0.0359	
Residual	0.0010	10	0.0001			
Lack of fit	0.0010	3	0.0003	77000.70	<0.0001	Significant
Pure error	2.940E-08	7	4.200E-09			
Cor. total	0.1084	19				

typically more resistant to changes in experimental circumstances, such as temperature and pH, which might influence the adsorption kinetics, and enables comparison of several adsorbents: non-linear models can be used to evaluate the adsorption kinetics and equilibrium adsorption capacities of various adsorbents.

In conclusion, compared to their linear counterparts, non-linear adsorption kinetics models, such as the pseudo-first-order, pseudo-second-order, intraparticle diffusion, and Elovich models, have several advantages. These advantages include improved experimental data fitting accuracy, information on the adsorption mechanism, predictive power, robustness to changes in experimental conditions, and the ability to compare various adsorbents.

3.7. Effect of temperature

Variable concentrations of water contaminants in aquatic solutions can have a significant impact on the effectiveness of adsorbents for treating contaminated water and wastewater. In this study, the concentrations of the examined water contaminants, MB and AR97, had a significant impact on their adsorption onto MOR at different ambient temperatures of 298, 308, 318, and 328 K. The data presented in the study clearly demonstrated that the amount of sorbed MB and AR97 was proportional to the increase in initial MB and AR97 concentration, as depicted in Fig. 8. The study also investigated the parameters of thermodynamics that were dependent on temperature.

Table 7 summarizes the results, including the $\Delta G°$, $\Delta S°$, and $\Delta H°$ values. The negative values of $\Delta G°$ at various temperatures controlled the spontaneity of the MB and AR97 adsorption process onto MOR. The spontaneity of the adsorption process was confirmed at higher temperatures by the increase in the negativity of the $\Delta G°$ values, and vice versa. The positive values of $\Delta S°$ justified the increase in system unpredictability at the solid–liquid interface [33–35].

Table 5
Parameters for the isothermal modeling of Acid Red 97 and methylene blue sorption onto MOR sorbent

Isotherm	Equations	Value of parameters	Methylene blue	Acid Red 97
Langmuir	$\frac{C_e}{q_e}=\frac{1}{q_m K_L}+\frac{C_e}{q_m}$	$q_{m,\exp}$ (mmol/g)	1.75	1.736
		q_m (mmol/g)	1.72	1.714
		K_L (L/mmol)	0.126	0.389
		R^2	0.999	0.998
Freundlich	$\ln q_e=\ln K_F+\frac{1}{n}\ln C_e$	n	1.3	1.66
		K_F (mmol/g)(L/mmol)$^{1/n}$	7.78	6.48
		R^2	0.7863	0.726
Dubinin–Radushkevich	$\ln q_e=\ln Q_{DR}-K_{DR}\varepsilon^2$	Q_{DR}	1.172	0.599
		K_{DR} (J^2/mol^2)	–1.667E-09	–1.537E-09
		E_a (kJ/mol)	18.84	40.65
		R^2	0.788	0.764
Temkin	$q_e=\beta_T\ln K_T+\beta_T\ln C_e$	β_T (L/mol)	11,482.63	61,326.4
		A_T (kJ/mol)	16.82	48.72
		R^2	0.8546	0.824

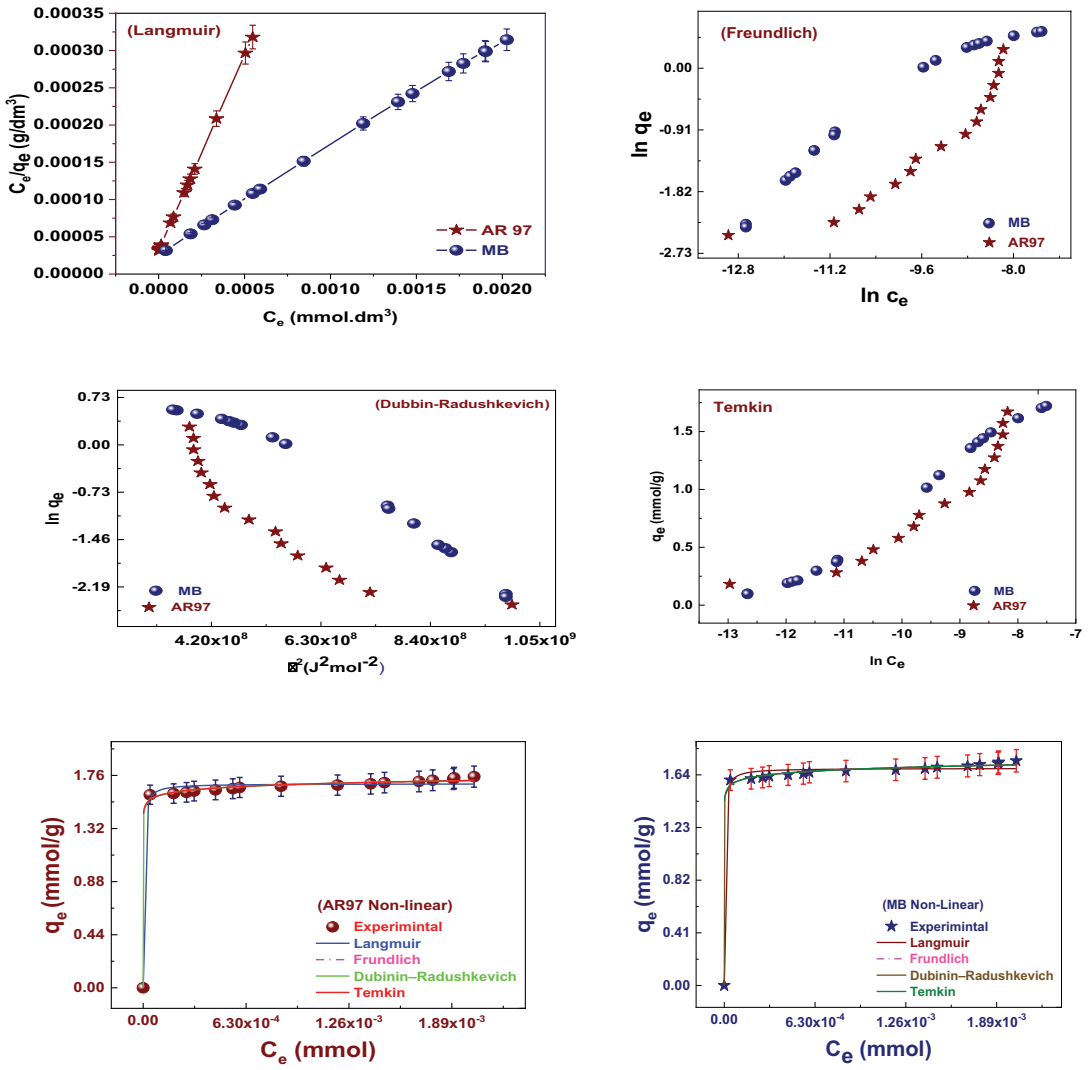

Fig. 6. Adsorption isotherm for Acid Red 97 and methylene blue.

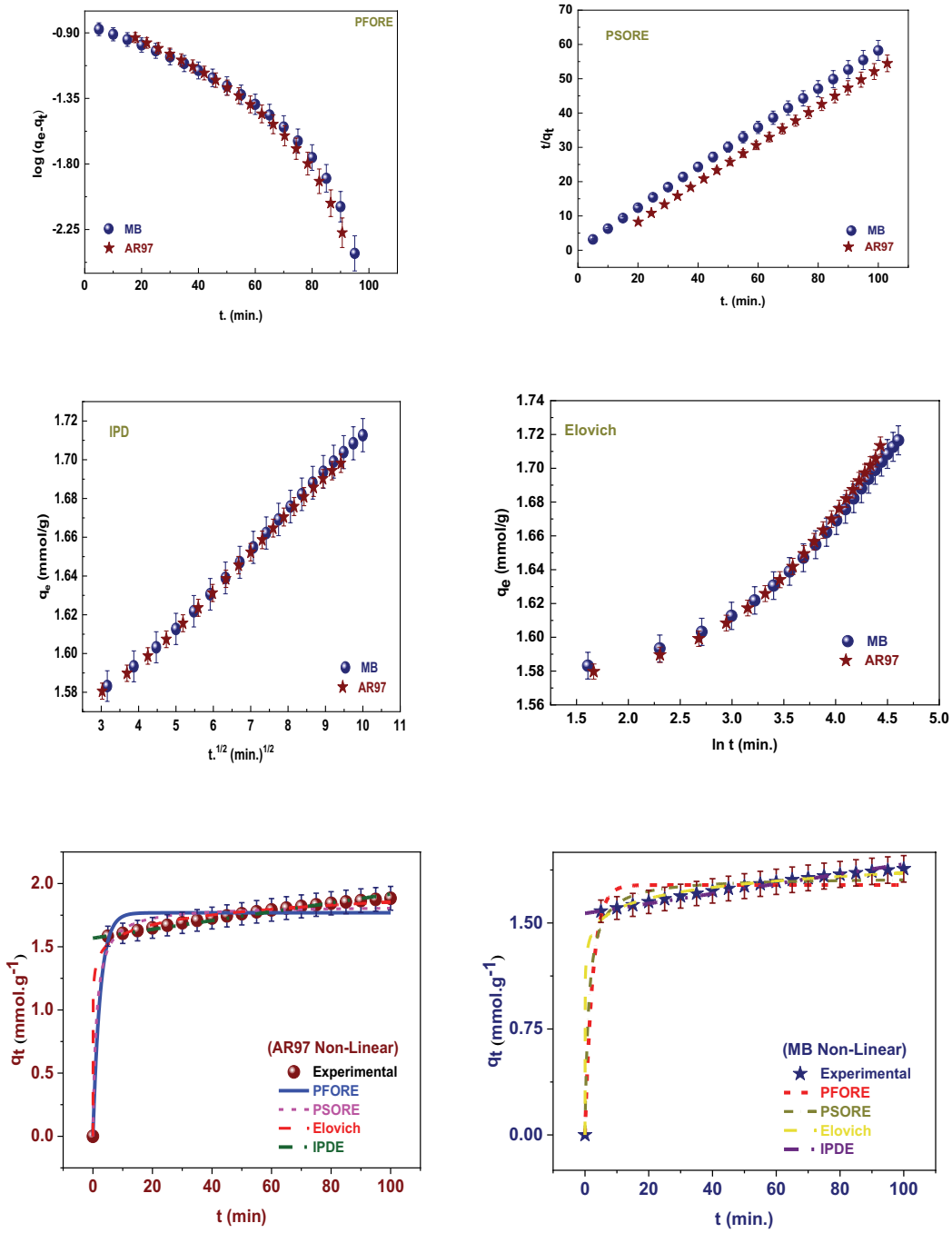

Fig. 7. Kinetic model of Acid Red 97 and methylene blue adsorption on MOR.

The Box–Behnken design, using temp., pH, and dose as X_1, X_2, and X_3, respectively, indicated that the optimum conditions for AR97 were pH 3 and time 100 min, with a dose of 0.01 g. The model was found to be significant, with a model *F*-value of 156.62. Model terms with *p*-values less than 0.0500 were considered significant. On the other hand, the best conditions for MB were found to be pH 9, dose 0.01 g, and time 100 min (Fig. 9). The model was also found to be significant, with a model *F*-value of 35.81. The study of the effect of temperature indicated that the reaction was spontaneous and endothermic, as the adsorption and removal efficiency increased with an increase in temperature, as shown in Tables 8 and 9.

3.8. Optimization of factors

Using the programmed Design-Expert 7.0, optimal values for the adsorption of AR97 and MB on MOR were predicted. In a typical design, the response factor was set to maximum, while the other three factors were set in a range from low (1) to high (+1). The favored solution with the greatest response was ultimately picked from the

Table 6
Kinetic modeling parameters of methylene blue@Acid Red 97 sorption onto MOR sorbent

Model	Equations	Value of parameters	Methylene blue	Acid Red 97
Pseudo-first-order kinetic	$\log(q_e - q_t) = \log q_e - \left(\frac{K_1}{2.303}\right)t$	K_1 (min^{-1})	0.14	0.0125
		q_e (mmol/g)	0.188	0.324
		R^2	0.898	0.882
Pseudo-second-order kinetic	$\frac{t}{q_t} = \frac{1}{K_2 q_e^2} + \frac{t}{q_e}$	K_2 (g/mg·min)	0.388	0.217
		q_e (mmol/g)	1.744	1.68
		R^2	0.999	0.999
Intraparticle diffusion	$q_t = K_i t^{1/2} + X$	K_i (mg/g·min$^{1/2}$)	–7.56	–7.057
		X (mg/g)	0.611	0.577
		R^2	0.766	0.745
Elovich	$q_t = \frac{1}{\beta}\ln(\alpha\beta) + \frac{1}{\beta}\ln t$	β (g/mg)	3.85	3.89
		α (mg/g·min)	2.96	2.79
		R^2	0.755	0.764
Experimental data		q_e (exp) (mmol/g)	1.716	1.705

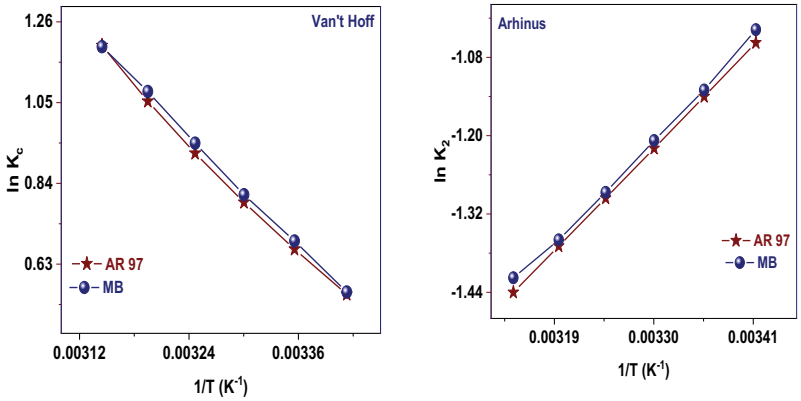

Fig. 8. Effect of temperature on adsorption of Acid Red 97 and methylene blue on MOR (a) van't Hoff and (b) Arrhenius.

Table 7
Thermodynamic parameter of adsorption of Acid Red 97 and methylene blue by MOR

Adsorbate	$\Delta H°$ (kJ/mol)	$\Delta S°$ (J/mol·K)	T_0 (K)	$-\Delta G°$ (kJ/mol)				
				293 K	298 K	303 K	308 K	318 K
Methylene blue	21.05	75.86	276.19	1.27	1.65	2.4	2.79	3.17
Acid Red 97	16.46	64.87	252.27	2.64	2.89	3.29	3.6	4.26

software-generated solutions. Table 10 provides examples of these projected values under ideal conditions and experimental values [36].

4. Mechanism of interaction

The rate of dye adsorption onto nano-adsorbent is influenced by several parameters, including pH, temperature, contact time, and dye concentration. A thorough investigation of how these parameters impact the adsorption rate is crucial in facilitating the understanding of the adsorption mechanisms. There are various physico-chemical adsorption mechanisms utilized for treating AR97 and MB dyes, including electrostatic interaction. AR97, being an anionic dye, has a negative charge on its surface during dissociation and is attracted to the positively charged surface of the adsorbent at pH lower than pH_{ZPC} 7.2, leading to adsorption at pH 3. In contrast, MB, being a cationic dye, has optimal adsorption at pH 10 as it has a positive charge during dissociation that is attracted to the negatively charged surface of the adsorbent at pH higher than pH_{ZPC}, signifying that it has a positive charge on its surface. Other mechanisms include hydrogen bond linkage, surface complexity, and Π–Π interaction, which are possible due to the presence of aromatic rings in both dyes.

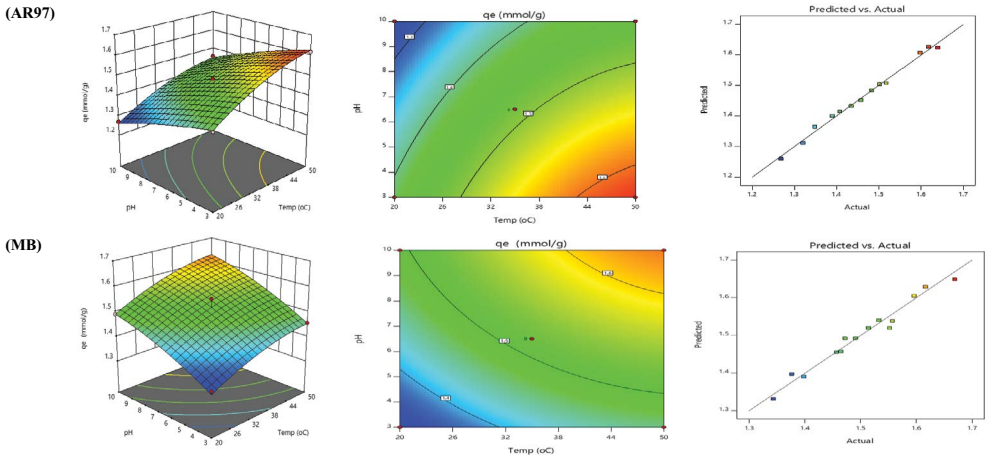

Fig. 9. Response surface plots and contour plots showing the impact of temperature on (a) Acid Red 97 and (b) methylene blue adsorption, respectively.

Table 8
Analysis of variance regarding the impact of time on methylene blue adsorption

Source	Sum of squares	df	Mean square	*F*-value	*p*-value	
Model	0.1602	9	0.0178	156.62	<0.0001	Significant
A-Temp.	0.0810	1	0.0810	712.74	<0.0001	
B-pH	0.0542	1	0.0542	476.50	<0.0001	
C-Dose	0.0176	1	0.0176	154.62	<0.0001	
AB	0.0001	1	0.0001	0.9405	0.3550	
AC	0.0000	1	0.0000	0.2415	0.6337	
BC	0.0007	1	0.0007	6.09	0.0333	
A^2	0.0056	1	0.0056	48.93	<0.0001	
B^2	0.0005	1	0.0005	4.23	0.0667	
C^2	0.0003	1	0.0003	2.61	0.1375	
Residual	0.0011	10	0.0001			
Lack of fit	0.0011	3	0.0004			
Pure error	0.0000	7	0.0000			
Cor. total	0.1614	19				

Table 9
Analysis of variance for Acid Red 97 adsorption as the effect of time

Source	Sum of squares	df	Mean square	*F*-value	*p*-value	
Model	0.1100	9	0.0122	35.81	<0.0001	Significant
A-Temp	0.0340	1	0.0340	99.75	<0.0001	
B-pH	0.0559	1	0.0559	163.88	<0.0001	
C-Dose	0.0142	1	0.0142	41.69	<0.0001	
AB	0.0000	1	0.0000	0.1130	0.7437	
AC	0.0003	1	0.0003	0.9059	0.3637	
BC	0.0006	1	0.0006	1.73	0.2172	
A^2	0.0025	1	0.0025	7.39	0.0216	
B^2	0.0016	1	0.0016	4.68	0.0559	
C^2	0.0005	1	0.0005	1.46	0.2548	
Residual	0.0034	10	0.0003			
Lack of fit	0.0022	3	0.0007			
Pure error	0.0013	7	0.0002			
Cor. total	0.1134	19				

Table 10
Optimal values for the adsorption of Acid Red 97 and methylene blue on MOR

Parameter	Dose (g)		Conc. (mmol)		pH		q_e (mmol/g)	
Dye	AR97	MB	AR97	MB	AR97	MB	AR97	MB
Predicted	0.01	0.01	0.0034	0.0197	3	10	1.68	1.62
Experimental	0.01	0.01	100		3	10	1.705	1716

Table 11
Comparison of adsorption of Acid Red 97 for MOR with different adsorbents

Adsorbent	q_m (mg/g)	References
HC	1,126.62	[37]
Zn_2Al-NO_3 LDHs	299.50	[38]
ABR	372.69	[39]
Activated carbon	554.35	[40]
Yemen natural clay	196.70	[41]
ABR	352.15	[42]
MOR	1,212.76	This search

Table 12
Comparison of adsorption of methylene blue for MOR with different adsorbents

Adsorbent	q_m (mg/g)	References
Neem sawdust	3.62	[43]
Beer brewery waste	4.92	[44]
Cow dung ash	5.31	[45]
Coir pith carbon	5.87	[46]
Orange peel	20.50	[47]
Activated olive stones	22.1	[48]
Cogon grass	27.40	[46]
Banana peel	29.94	[49]
Corn husk	30.33	[50]
Cu-BTC 143.27	143.27	[50]
HKUST-1/GO	140	[51]
ZIF-8	522.95	[35]
MOR	559.8	This work

5. Comparison with another adsorbent

The adsorption capacity of MOR compared to those reported in the literature is presented in Table 11 for the adsorption of AR97 and Table 12 for the adsorption of MB. Based on this comparison, MOR provides the highest adsorption capacity reported to date for the adsorption of AR97 and MB dyes. This finding suggests that the prepared adsorbent could be a potential candidate for the efficient removal of acidic dyes from aqueous solutions.

6. Conclusion

The objective of this research was to explore the potential of MOR (modified orange residue) in enhancing the adsorption of both cationic (methylene blue) and anionic dyes (Acid Red 97). The study used Box–Behnken design and response surface methods to determine the most effective experimental setups for increased dye removal. Three variables, including pH of the solution, amount of dye present, and mass ratio of MOR, were selected and their impact on adsorption of AR97 and MB was analyzed. The results indicated that all three parameters played a significant role in the adsorption process. It was observed that the mass ratio of MOR had a greater influence on AR97 adsorption than on MB adsorption. In contrast to MB adsorption, the adsorption of AR97 was found to be more sensitive to the concentration of the dye in the solution. Furthermore, the study revealed that the interaction between solution pH and dye concentration had a greater impact on AR97 adsorption compared to MB adsorption. The analysis of linear-by-linear interactions indicated that the interaction between dye concentration and mass ratio of mordenite had a more significant influence on MB adsorption compared to AR97 adsorption. The study found that at low dye concentrations, the mass ratio of MOR had a greater impact on MB adsorption. On the other hand, the adsorption of AR97 was highly dependent on its concentration in solution at low pH levels. The analysis of the adsorption isotherm, which was kinetically fitted to the pseudo-second-order, indicated that the adsorption process was chemisorption, as the binding energies for both dyes were greater than 8 kJ/mol. The thermodynamic analysis confirmed that the reaction was endothermic and spontaneous, and the adsorption capacity increased with the rise in temperature.

Acknowledgement

Princess Nourah bint Abdulrahman University Researchers Supporting Project number (PNURSP2023R92), Princess Nourah bint Abdulrahman University, Riyadh, Saudi Arabia.

References

[1] J. Acharya, J. Sahu, C. Mohanty, B. Meikap, Removal of lead(II) from wastewater by activated carbon developed from *Tamarind wood* by zinc chloride activation, Chem. Eng. J., 149 (2009) 249–262.
[2] S. Banerjee, M.C. Chattopadhyaya, Adsorption characteristics for the removal of a toxic dye, tartrazine from aqueous solutions by a low-cost agricultural by-product, Arabian J. Chem., 10 (2017) S1629–S1638.
[3] M.A. El-Bindary, M.G. El-Desouky, A.A. El-Bindary, Adsorption of industrial dye from aqueous solutions onto thermally treated green adsorbent: a complete batch system evaluation, J. Mol. Liq., 346 (2021) 117082, doi: 10.1016/j.molliq.2021.117082.

[4] C. Aharoni, M. Ungarish, Kinetics of activated chemisorption. Part 2.—Theoretical models, J. Chem. Soc., Faraday Trans. 1 F, 73 (1977) 456–464.
[5] G.H. Al-Hazmi, A.M.A. Adam, M.G. El-Desouky, A.A. El-Bindary, A.M. Alsuhaibani, M.S. Refat, Efficient adsorption of Rhodamine B using a composite of Fe_3O_4@ZIF-8: synthesis, characterization, modeling analysis, statistical physics and mechanism of interaction, Bull. Chem. Soc. Ethiop., 37 (2023) 211–229.
[6] M.G. El-Desouky, M.A. Khalil, A.A. El-Bindary, M.A. El-Bindary, Biological, biochemical and thermochemical techniques for biofuel production: an updated review, Biointerface Res. Appl. Chem., 12 (2022) 3034–3054.
[7] N. Hassan, A. Shahat, A. El-Didamony, M.G. El-Desouky, A.A. El-Bindary, Equilibrium, kinetic and thermodynamic studies of adsorption of cationic dyes from aqueous solution using ZIF-8, Moroccan J. Chem., 8 (2020) 2627–2637.
[8] M.A. Ahmad, N.K. Rahman, Equilibrium, kinetics and thermodynamic of Remazol Brilliant Orange 3R dye adsorption on coffee husk-based activated carbon, Chem. Eng. J., 170 (2011) 154–161.
[9] F.A. Batzias, D.K. Sidiras, Simulation of dye adsorption by beech sawdust as affected by pH, J. Hazard. Mater., 141 (2007) 668–679.
[10] M. Auta, B.H. Hameed, Optimized waste tea activated carbon for adsorption of methylene blue and Acid Blue 29 dyes using response surface methodology, Chem. Eng. J., 175 (2011) 233–243.
[11] G.A.A. Al-Hazmi, A.A. El-Zahhar, M.G. El-Desouky, M.A. El-Bindary, A.A. El-Bindary, Efficiency of Fe_3O_4@ZIF-8 for the removal of doxorubicin from aqueous solutions: equilibrium, kinetics and thermodynamic studies, Environ. Technol., (2022) 1–20, doi: 10.1080/09593330.2022.2121181.
[12] G.A.A. Al-Hazmi, A.A. El-Zahhar, M.G. El-Desouky, A. El-Bindary, Superior adsorption and removal of doxorubicin from aqueous solution using activated carbon via thermally treated green adsorbent: isothermal, kinetic, and thermodynamic studies, Environ. Technol., (2022) 1–20, doi: 10.1080/09593330.2022.2159540.
[13] Y.S. Al-Degs, M.I. El-Barghouthi, A.H. El-Sheikh, G.M. Walker, Effect of solution pH, ionic strength, and temperature on adsorption behavior of reactive dyes on activated carbon, Dyes Pigm., 77 (2008) 16–23.
[14] Z.A. AlOthman, M.A. Habila, R. Ali, A.A. Ghafar, M.S. El-din Hassouna, Valorization of two waste streams into activated carbon and studying its adsorption kinetics, equilibrium isotherms and thermodynamics for methylene blue removal, Arabian J. Chem., 7 (2014) 1148–1158.
[15] A.H. Jawad, N.N.A. Malek, A.S. Abdulhameed, R. Razuan, Synthesis of magnetic chitosan-fly ash/Fe_3O_4 composite for adsorption of Reactive Orange 16 dye: optimization by Box–Behnken design, J. Polym. Environ., 28 (2020) 1068–1082.
[16] W. Boumya, M. Khnifira, A. Machrouhi, M. Abdennouri, M. Achak, S. Qourzal, H. Tounsadi, N. Barka, Box–Behnken design for understanding of adsorption behaviors of cationic and anionic dyes by activated carbon, Desal. Water Treat., 212 (2021) 204–211.
[17] H. Mirhosseini, T. Shamspur, A. Mostafavi, Novel adsorbent g-C_3N_4/ZnV_2O_4 for efficient removal of crystal violet dye: removal process optimization, adsorption isotherms, and kinetic modeling, Appl. Organomet. Chem., 36 (2022) e6867, doi: 10.1002/aoc.6867.
[18] N.M. El-Metwaly, H.A. Katouah, M.G. El-Desouky, A.A. El-Bindary, M.A. El-Bindary, Fabricating of Fe_3O_4@Ag-MOF nanocomposite and evaluating its adsorption activity for removal of doxorubicin, J. Environ. Sci. Health, Part A, 57 (2022) 1099–1115.
[19] I. Langmuir, The constitution and fundamental properties of solids and liquids. Part I. Solids, J. Am. Chem. Soc., 38 (1916) 2221–2295.
[20] H.M.F. Freundlich, Over the adsorption in solution, J. Phys. Chem., 57 (1906) 385–471.
[21] M.M. Dubinin, L.V. Radushkevich, Equation of the characteristic curve of activated charcoal, Proc. Acad. Sci. USSR Phys. Chem. Sect., 55 (1947) 331–333.
[22] M.J. Tempkin, V. Pyzhev, Kinetics of ammonia synthesis on promoted iron catalyst, Acta Phys. Chim. USSR, 12 (1940) 327–356.
[23] M.G. El-Desouky, A.A. El-Bindary, Magnetic metal-organic framework (Fe_3O_4@ZIF-8) nanocomposites for adsorption of anionic dyes from wastewater, Inorg. Nano-Metal Chem., (2021) 1–15, doi: 10.1080/24701556.2021.2007131.
[24] G.A.A. Al-Hazmi, M.A. El-Bindary, M.G. El-Desouky, A.A. El-Bindary, Efficient adsorptive removal of industrial dye from aqueous solution by synthesized zeolitic imidazolate framework-8 loaded date seed activated carbon and statistical physics modeling, Desal. Water Treat., 258 (2022) 85–103.
[25] G.H. Al-Hazmi, M.G. El-Desouky, A.A. El-Bindary, Synthesis, characterization and microstructural evaluation of ZnO nanoparticles by William-Hall and size-strain plot methods, Bull. Chem. Soc. Ethiop., 36 (2022) 815–829.
[26] S. Lagergren, About the theory of so-called adsorption of soluble substances, Sven. Vetenskapsakad. Handingarl, 24 (1898) 1–39.
[27] Y.-S. Ho, G. McKay, Pseudo-second-order model for sorption processes, Process Biochem., 34 (1999) 451–465.
[28] F.-C. Wu, R.-L. Tseng, R.-S. Juang, Initial behavior of intraparticle diffusion model used in the description of adsorption kinetics, Chem. Eng. J., 153 (2009) 1–8.
[29] J. Zeldowitsch, The catalytic oxidation of carbon monoxide on manganese dioxide, Acta Physicochim. URSS, 1 (1934) 364–449.
[30] T.A. Altalhi, M.M. Ibrahim, G.A.M. Mersal, M.H.H. Mahmoud, T. Kumeria, M.G. El-Desouky, A.A. El-Bindary, M.A. El-Bindary, Adsorption of doxorubicin hydrochloride onto thermally treated green adsorbent: equilibrium, kinetic and thermodynamic studies, J. Mol. Struct., 1263 (2022) 133160, doi: 10.1016/j.molstruc.2022.133160.
[31] M.A. El-Bindary, M.G. El-Desouky, A.A. El-Bindary, Metal–organic frameworks encapsulated with an anticancer compound as drug delivery system: synthesis, characterization, antioxidant, anticancer, antibacterial and molecular docking investigation, Appl. Organomet. Chem., 36 (2022) e6660, doi: 10.1002/aoc.6660.
[32] M.G. El-Desouky, A.A. El-Bindary, M.A.M. El-Afify, N. Hassan, Synthesis, characterization, theoretical calculation, DNA binding, molecular docking, anticovid-19 and anticancer chelation studies of some transition metal complexes, Inorg. Nano-Metal Chem., 52 (2022) 1273–1288.
[33] G.A.A. AlHazmi, Kh. S. AbouMelha, M.G. El-Desouky, A.A. El-Bindary, Effective adsorption of doxorubicin hydrochloride on zirconium metal-organic framework: equilibrium, kinetic and thermodynamic studies, J. Mol. Struct., 1258 (2022) 132679, doi: 10.1016/j.molstruc.2022.132679.
[34] M.G. El-Desouky, A.A. El-Bindary, M.A. El-Bindary, Low-temperature adsorption study of carbon dioxide on porous magnetite nanospheres iron oxide, Biointerface Res. Appl. Chem., 12 (2021) 6252–6268.
[35] A.S. Al-Wasidi, I.I.S. AlZahrani, A.M. Naglah, M.G. El-Desouky, M.A. Khalil, A.A. El-Bindary, M.A. El-Bindary., Effective removal of methylene blue from aqueous solution using metal-organic framework; modeling analysis, statistical physics treatment and DFT calculations, ChemistrySelect, 6 (2021) 11431–11447.
[36] A. Mulay, V.K. Rathod, Ultrasound-assisted synthesis of ethyl hexanoate using heterogeneous catalyst: optimization using Box–Behnken design, 99 (2022) 100573, doi: 10.1016/j.jics.2022.100573.
[37] I. Chouaybi, H. Ouassif, M. Bettach, E.M. Moujahid, Fast and high removal of Acid Red 97 dye from aqueous solution by adsorption onto a synthetic hydrocalumite: structural characterization and retention mechanisms, Inorg. Chem. Commun., 146 (2022) 110169, doi: 10.1016/j.inoche.2022.110169.

[38] T. Xue, Y. Gao, Z. Zhang, A. Umar, X. Yan, X. Zhang, Z. Guo, Q. Wang, Adsorption of acid red from dye wastewater by Zn_2Al-NO_3 LDHs and the resource of adsorbent sludge as nanofiller for polypropylene, J. Alloys Compd., 587 (2014) 99–104.
[39] F.C. Drumm, D.S.P. Franco, J. Georgin, P. Grassi, S.L. Jahn, G.L. Dotto, Macro-fungal (*Agaricus bisporus*) wastes as an adsorbent in the removal of the Acid Red 97 and crystal violet dyes from ideal colored effluents, Environ. Sci. Pollut. Res., 28 (2021) 405–415.
[40] V. Gómez, M.S. Larrechi, M.P. Callao, Kinetic and adsorption study of acid dye removal using activated carbon, Chemosphere, 69 (2007) 1151–1158.
[41] A. Al-Wahbi, Adsorption of Diazo Dye C.I. Acid Red 97 from aqueous solution onto Yemen natural clay: equilibrium and thermodynamic studies, Jordanian J. Eng. Chem. Ind. (JJECI), 1 (2018) 1–11.
[42] F. Aouaini, L. Sellaoui, M.M. Alanazi, G.L. Dotto, W. Alfwzan, H.A. Al-Yousef, A. Erto, Theoretical analysis of the removal mechanism of Crystal Violet and Acid Red 97 dyes on *Agaricus bisporus* residue, J. Mol. Liq., 343 (2021) 117621, doi: 10.1016/j.molliq.2021.117621.
[43] S. Khattri, M.K. Singh, Colour removal from synthetic dye wastewater using a bioadsorbent, Water Air Soil Pollut., 120 (2000) 283–294.
[44] W.-T. Tsai, H.-C. Hsu, T.-Y. Su, K.-Y. Lin, C.-M. Lin, Removal of basic dye (methylene blue) from wastewaters utilizing beer brewery waste, J. Hazard. Mater., 154 (2008) 73–78.
[45] F. Ayca Ozdemir, B. Demirata, R. Apak, Adsorptive removal of methylene blue from simulated dyeing wastewater with melamine-formaldehyde-urea resin, J. Appl. Polym. Sci., 112 (2009) 3442–3448.
[46] D. Kavitha, C. Namasivayam, Experimental and kinetic studies on methylene blue adsorption by coir pith carbon, Bioresour. Technol., 98 (2007) 14–21.
[47] E.O. Akperov, O.H. Akperov, The wastage of the cotton stalks (*Gossypium hirsutum* L.) as low-cost adsorbent for removal of the Basic Green 5 dye from aqueous solutions, Appl. Water Sci., 9 (2019) 1–9.
[48] G. Annadurai, R.-S. Juang, D.-J. Lee, Use of cellulose-based wastes for adsorption of dyes from aqueous solutions, J. Hazard. Mater., 92 (2002) 263–274.
[49] J. Hu, W. Dai, X. Yan, Comparison study on the adsorption performance of methylene blue and Congo red on Cu-BTC, Desal. Water Treat., 57 (2016) 4081–4089.
[50] L. Li, X.L. Liu, H.Y. Geng, B. Hu, G.W. Song, Z.S. Xu, A MOF/graphite oxide hybrid (MOF: HKUST-1) material for the adsorption of methylene blue from aqueous solution, J. Mater. Chem. A, 1 (2013) 10292–10299.
[51] Uma, S. Banerjee, Y.C. Sharma, Equilibrium and kinetic studies for removal of malachite green from aqueous solution by a low cost activated carbon, J. Ind. Eng. Chem., 19 (2013) 1099–1105.

Supporting information

S1. Adsorption isotherm

Isotherm studies give significant visions by clarifying the adsorbate distribution between solid and solution phase during the adsorption equilibrium, and adsorption isotherms expose the behavior of adsorbate how to interact with adsorbent. Equilibrium revisions that give the capacity of the adsorbent and adsorbate are described by adsorption isotherms, which is usually the ratio between the quantity adsorbed and that remained in solution at equilibrium at fixed temperature. Numerous isotherm models have been used for considering the equilibrium adsorption of compounds from solutions such as Langmuir, Freundlich, Dubinin–Radushkevich and Temkin.

The Langmuir isotherm model accepts the uniform energies of adsorption onto the adsorbent surface. It is based on statement of the existence of monolayer adsorption onto a completely homogeneous surface with a fixed number of identical sites and with negligible interaction between adsorbed molecules. The Freundlich model is an empirical equation based on adsorption of heterogeneous surface or surface supporting sites of varied affinities. It is assumed that the stronger binding sites are occupied first, and that the binding strength decreases with the increasing degree of site occupation. Dubinin–Radushkevich isotherm is an empirical model initially for the adsorption of subcritical vapors onto micropore solids following a pore filling mechanism. It is applied to distinguish the physical and chemical adsorption for removing a molecule from its location in the sorption space to the infinity. The Temkin isotherm assumes that the heat of adsorption of all molecules in the phase decreases linearly when the layer is covered and that the adsorption has a maximum energy distribution of uniform bond.

The linear and non-linear forms of Langmuir, Freundlich, Dubinin–Radushkevich and Temkin isotherm models and their parameters are shown in Table S1 where q_e the adsorbed amount of dye at equilibrium concentration (mmol/g), q_{mL} is the maximum sorption capacity (corresponding to the saturation of the monolayer, mmol/g) and K_L is the Langmuir binding constant which is related to the energy of sorption (L/mmol), C_e is the equilibrium concentration of dyes in solution (M). K_F (mmol/g)(L/mmol)$^{1/n}$ and n are the Freundlich constants related to the sorption capacity and intensity, respectively. K_{DR} (J^2/mol^2) is a constant related to the sorption energy, Q_{DR} (mmol/g) is the theoretical saturation capacity, ε (J^2/mol^2) is the Polanyi potential. R (8.314 J/mol·K) is the gas constant, T is the temperature where the adsorption occurs, A_T (L/mg) is the Temkin isotherm constant, b_T (J/mol) is Temkin constant in relation to heat of adsorption.

S2. Adsorption kinetics

The study of adsorption kinetics describes the solute uptake rate and evidently this rate controls the residence time of adsorbate uptake at the solid-solution interface. The rate of removal of tested dye by adsorption was rapid initially and then slowed gradually until it attained an equilibrium beyond which there was significant increase in the rate of removal Table S2.

where q_t is the amount of dye adsorbed (mg/g) at various times t, q_e is the maximum adsorption capacity (mg/g) for pseudo-first-order adsorption, K_1 is the pseudo-first-order rate constant for the adsorption process (min^{-1}), q_2 is the maximum adsorption capacity (mg/g) for the pseudo-second-order adsorption, K_2 is the rate constant of pseudo-second-order adsorption (g/mg·min). The straight-line plots of $\log(q_e - q_t)$ vs. t for the pseudo-first-order reaction and t/q_t vs. t for the pseudo-second-order reaction.

Since neither the pseudo-first-order nor the pseudo-second-order model can identify the diffusion mechanism, the kinetic results were further analyzed for diffusion mechanism by using the intraparticle diffusion model. The effect of intraparticle diffusion constant (internal surface and

Table S1
Isotherms and their linear forms for the adsorption

Isotherm	Equation	
Langmuir	$\frac{C_e}{q_e}=\frac{1}{q_m K_L}+\frac{C_e}{q_m}$	Constants q_m and K_L are calculated by the plot of C_e/q_e vs. C_e with slope $1/q_m$ and intercept $1/(q_m K_L)$
Freundlich	$\ln q_e=\ln K_F+\frac{1}{n}\ln C_e$	K_F and n can be calculated from a linear plot of $\ln q_e$ vs. $\ln C_e$
Dubinin–Radushkevich	$\ln q_e=\ln Q_{DR}-K_{DR}\varepsilon^2$	Slope of the plot of $\ln q_e$ vs. ε^2 gives K_{DR} (mol²/kJ²) and the intercept yields the adsorption capacity, Q_{DR} (mmol/g)
Temkin	$q_e=\beta_T \ln K_T+\beta_T \ln C_e$	Parameters β and K_T are the Temkin constants that can be determined by the plot of q_e vs. $\ln C_e$

Table S2
Kinetic parameters and their correlation coefficients for the adsorption

Model	Equation	
Pseudo-first-order kinetic	$\log(q_e-q_t)=\log q_e-\left(\frac{K_1}{2.303}\right)t$	Plot of $\ln(q_e-q_t)$ against t gives a straight line with the slope $-K_1$ and intercept $\ln q_e$
Pseudo-second-order kinetic	$\frac{t}{q_t}=\frac{1}{K_2 q_e^2}+\frac{t}{q_e}$	Values of K_2 and q_e for different initial concentrations of dye were calculated from the slope and intercept of the linear plot of t/q_t vs. t
Intraparticle diffusion	$q_t=K_i t^{1/2}+X$	Parameters K_{dif} and C were determined from the linear plot of q_t vs. $t^{1/2}$
Elovich	$q_t=\frac{1}{\beta}\ln(\alpha\beta)+\frac{1}{\beta}\ln t$	Constants α and β were obtained from the slope and intercept of a line plot of q_t vs. $\ln t$

pore diffusion) on adsorption can be determined by the following Eq. (7).
where I is the intercept and k_{id} is the rate constant of intraparticle diffusion (mg/g·min$^{1/2}$) which is determined from the linear plot of q_t vs. $t^{1/2}$, and it is usually used to compare mass transfer rates. According to this model, the plot of uptake, q_t, vs. the square root of time, $t^{1/2}$ should be linear if intraparticle diffusion is involved in the adsorption process and if these lines pass through the origin, then intraparticle diffusion is the rate controlling step. The intraparticle diffusion rate constant and intercept values are displayed in (Table S2).

The Elovich equation is used for general application to chemical adsorption. The equation has been applied satisfactorily to some chemical adsorption processes and has been found to cover a wide range of slow adsorption rates. The same equation is often valid for systems in which the adsorbing surface is heterogeneous, and is formulated as Eq. (8):
where α is the chemical adsorption rate (mg/mg·min) and β is a coefficient in relation with the extension of covered surface and activation energy of chemical adsorption (g/mg). Plot of q_t vs. $\ln t$ gave a linear relationship with slope of (1/β) and an intercept of (1/β) ln(αβ). The 1/β value reflects the number of sites available for adsorption whereas the value of (1/β) ln(αβ) indicates the adsorption quantity when $\ln t$ equal to zero.

Thermodynamic

It is important to investigate the effect of temperature on adsorption in a view of practical application. The adsorption experiments were carried out at different temperatures. The behavior confirms that the adsorption process if it endothermic or exothermic. This observation can be attributed to increasing of the mobility of the adsorbate molecules and rate of diffusion of adsorbate molecules across the surface of adsorbent with increasing temperature, which leads to an increase in the adsorption capacity. The adsorption equilibrium constant, K_c was determined [Eq. (9)] and used with the van't Hoff equation [Eq. (10)] and conventional thermodynamic equation [Eq. (11)] for evaluating the thermodynamic constants of the sorbents (i.e., the standard enthalpy change, $\Delta H°$, the standard free Gibbs energy, $\Delta G°$, and the standard entropy change, $\Delta S°$).

$$K_c=\frac{q_e}{C_e} \tag{9}$$

where q_e and C_e are equilibrium concentrations of CV and MG on the adsorbent and in the solution, respectively.

$$\Delta G°=-RT\ln K_c \tag{10}$$

$$\Delta G°=\Delta H°-T\Delta S° \tag{11}$$

Therefore, the van't Hoff equation becomes:

$$\ln K_c = \frac{-\Delta H^\circ}{RT} + \frac{\Delta S^\circ}{R} \quad (12)$$

The value of standard enthalpy change (ΔH°) and standard entropy change (ΔS°) for the adsorption process are thus determined from the slope and intercept of the plot of $\ln K_c$ vs. $1/T$.

Table S3
List of abbreviation

Symbol	Definition
q_e	Adsorbed amount of dye at equilibrium concentration, mmol/g
q_{mL}	Maximum sorption capacity (corresponding to the saturation of the monolayer, mmol/g)
K_L	Langmuir binding constant which is related to the energy of sorption, L/mmol
C_e	Equilibrium concentration of dyes in solution
K_F	Freundlich constants related to the sorption capacity, (mmol/g)(L/mmol)$^{1/n}$
n	Intensity
K_{DR}	Constant related to the sorption energy, J^2/mol^2
Q_{DR}	Theoretical saturation capacity, mmol/g
ε	Polanyi potential, J^2/mol^2
R	Gas constant, 8.314 J/mol·K
T	Temperature where the adsorption occurs
A_T	Temkin isotherm constant
b_T	Temkin constant in relation to heat of adsorption, J/mol
q_t	Amount of dye adsorbed, mmol/g
K_1	Rate constant for pseudo-first-order constant for the adsorption processes, min^{-1}
q_2	Maximum adsorption capacity for pseudo-second-order
K_2	Rate constant for pseudo-first-order constant for the adsorption processes, g/mg·min
α	Chemical adsorption rate, mg/g·min
β	Coefficient in relation with extension of covered surface
ΔG°	Free Gibb's energy
ΔH°	Enthalpy
ΔS°	Entropy
K_c	Distribution coefficient
C_{eq}	Concentration at equilibrium, mg/L